Letter

Unlimited number of spanning clusters in three-dimensional percolation above the critical point

Carlos G. L. Sousa,[1] José S. Andrade, Jr.,[1] André A. Moreira,[1] Cesar I. N. Sampaio Filho,[1] Erika Eiser,[2] Alex Hansen,[2] and Hans J. Herrmann[1,3,*]

[1]*Departamento de Física, Universidade Federal do Ceará, Caixa Postal 6030, Campus do Pici, 60455-760 Fortaleza, Ceará, Brazil*

[2]*PoreLab, Department of Physics, Norwegian University of Science and Technology, NO-7491 Trondheim, Norway*

[3]*ESPCI, PMMH, Paris, 7 quai St. Bernard, 75005, France*

(Received 21 November 2024; accepted 1 April 2025; published 16 June 2025)

Inspired by the formation of bigels, we developed a bond percolation model that yields multiple percolating clusters in three dimensions not only at the critical point, but also above it. Our simulations suggest that, in the thermodynamic limit, there is no upper limit to the number of percolating clusters. We show that in finite systems the maximum number of percolating clusters that can be obtained grows logarithmically with the lattice size. For equal initial densities in the thermodynamic limit, all clusters percolate at the same threshold and exhibit critical exponents consistent with the critical exponents of standard percolation. The threshold depends linearly on the initial density of species and the maximum and minimum initial densities decay exponentially with the maximal number of spanning clusters.

DOI: 10.1103/PhysRevResearch.7.L022067

Colloidal gels arise from the interplay between phase separation and arrest, resulting in space-spanning structures [1]. This has led to the discovery of a novel class of materials called "bigels." They are formed through arrested demixing in binary colloidal mixtures by tuning the interspecies interactions which results in the simultaneous formation of two spanning clusters, defined as those which connect different boundary segments. These bigels were visualized experimentally through confocal microscopy and simulated numerically [2,3]. Other studies also revealed experimental examples of bipercolated [4,5] and tripercolated structures [6,7]. Inspired by these experimental observations, it is therefore interesting to develop percolation models that can display multiple spanning percolation clusters, as the ones depicted in Fig. 1.

At first glance, results such as these seem to contradict a theorem [8] which states that, in any dimension d, in the thermodynamic limit above the critical point, there exists exactly one spanning cluster, while below the critical point, there are none. At the percolation threshold p_c one must distinguish between infinite and spanning clusters [9,10]. It was proven that the number of infinite clusters can only be either zero, one, or infinity [11,12]. In the case of spanning clusters, for $d > 1$, the probability of finding more than one spanning cluster at the critical point p_c does not go to zero as $L \to \infty$ [8]. In fact, for $d = 2$, an exact result for the probability of having k spanning clusters in two dimensions was derived using conformal invariance [13]. In another study [14], the go-with-the-winners strategy [15] was applied to a rectangular lattice with periodic boundaries in one direction to simulate five spanning clusters separated for two sites [16], and calculate the probability of obtaining them.

To achieve more than one percolating cluster above the critical point, the polychromatic model was introduced [17], where nodes or bonds are differentiated by species, enabling multiple percolating clusters, though constrained by the critical threshold of site percolation p_c. This concept was expanded upon with species-dependent bond models [18–20], correlated two-component percolation [21], site percolation with independent concentrations [22], AB percolation [23,24], colored percolation [25], two-color percolation [26], polychromatic random networks [27], and tricolor self-avoiding walks [28].

However, none of these models can obtain more than $1/p_c$ percolating clusters. The aim of our work is to present a model essentially based on bond percolation rules that allows for the occurrence of an arbitrary number of spanning clusters not only at the critical point but also above it. We seek to identify the necessary conditions to achieve k simultaneously spanning clusters and determine what limits the number of percolating clusters. Furthermore, we will analyze the structure of these clusters.

We consider a simple cubic lattice of size L, where initially all bonds are empty ($p = 0$) and a fraction $k\rho \leqslant 1$ of sites are randomly and permanently inhabited by k different species. Precisely, at the beginning, each species inhabits an equal fraction ρ of the sites of the lattice, with the constraint that no site can be inhabited by more than one species. Note that here we use the terms "empty" and "occupied" for bonds and "inhabited" and "uninhabited" for sites. Then, as in bond percolation [29], one starts to randomly select bonds and to occupy them, while ensuring that every bond can only be chosen once. When a chosen bond connects a site inhabited by a given species with an uninhabited site, then this site and

*Contact author: hans@fisica.ufc.br

Published by the American Physical Society under the terms of the Creative Commons Attribution 4.0 International license. Further distribution of this work must maintain attribution to the author(s) and the published article's title, journal citation, and DOI.

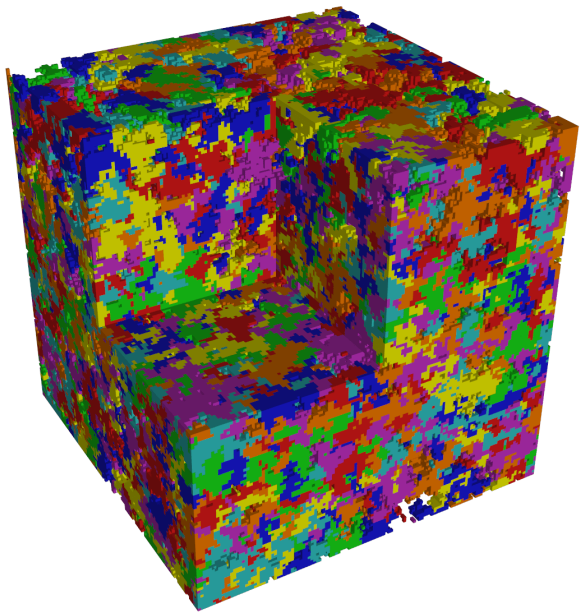


FIG. 1. Final configuration resulting from the simulation of our model in a cubic lattice with side length $L = 128$ and seven distinct species, $k = 7$. The different colors correspond to the seven percolating clusters associated with each species, which have been accommodated within the finite system. Note that the empty (uncolored) spaces between the colored clusters do not percolate by the end of the bond allocation process.

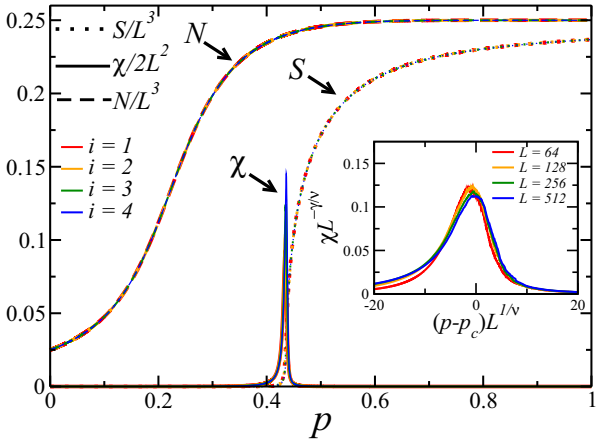


FIG. 2. Evolution of properties of the cluster distribution during the occupation process. Species are labeled in the order of percolation, that is, we label by 1 the species that first percolates, by 2 the second species to percolate, and so on. The curves are the average over 1000 samples. The colors indicate the order i in which the species percolated. The dotted lines correspond to the average size S of the largest cluster, the solid lines indicate the second moment of the cluster size distribution χ, as defined in Eq. (1), and the dashed lines indicate the number of nodes N that have been occupied by each species. For convenience, each of the quantities is scaled by the system size, as indicated in the figure's legend. We used a system size $L = 512$, with four species, and initial density $\rho = 0.025$. The inset shows the finite-size scaling of χ for the first percolating cluster using $p_c = 0.434$ and the critical exponents for 3D percolation.

all the uninhabited sites that may belong to its cluster will become inhabited by the same species. A cluster is defined here as a group of connected sites that are either uninhabited or inhabited by one single species. This rule allows the expansion of a species into uninhabited territory through the aggregation of clusters. A final and crucial rule is that if two neighboring sites are inhabited by different species, they retain their species identities even if they are connected by an occupied bond. Section I of the Supplemental Material [30] illustrates the rules of the model. In summary, this model generates clusters by growing distinct species through bond percolation, while preserving species boundaries. The case $k = 1$ is equivalent to standard percolation, while $\rho k = 1$ corresponds to the polychromatic model [17].

We implement periodic boundary conditions in directions x and y and open boundaries in the z direction. We define n_b as the number of bonds that have been chosen, therefore the probability of a bond occupation is $p = n_b/(3L^3 - L^2)$ which will be the variable controlling the percolation process. The properties of the model will be investigated as a function of two parameters, namely, the number of different species k and the density ρ of nodes initially inhabited by each species, and only the case in which the initial density ρ is the same for all species will be considered.

We search for percolating clusters that span from the top to the bottom of the cubic lattice along the z axis. Growing clusters of different species act as obstacles to one another. In this way, each species races to first reach the uninhabited nodes while blocking the growth of the competing clusters of other species.

In some cases, it is also possible to observe more than one percolating cluster of the same species. For example, for $\rho = 0.025$, $L = 512$, and $k = 4$, we observe with a probability of approximately 0.47 at least two percolating clusters of the same species at the critical point. Most of these spanning clusters of same species will merge to a single cluster with increasing p before the end of the occupation processes. However, in some cases, it is possible to observe two percolating clusters of the same species at $p = 1$. For instance, for $\rho = 3.89 \times 10^{-4}$, $L = 512$, and $k = 9$, this happens for about 2% of the samples.

Next, we investigate the evolution of cluster properties in our model. For this, we define S_i as the average number of nodes in the largest cluster of the ith species to percolate, the total number N_i of nodes inhabited by this species, and the second moment χ_i of the cluster-size distribution that is defined here as [31]

$$\chi_i = \frac{\sum_l s_{li}^2 - S_i^2}{N_i}, \tag{1}$$

where s_{li} is the mass of a cluster l inhabited by the ith species to percolate. Figure 2 illustrates the evolution of the cluster properties and the inset shows that the curves of the second moment χ for different values of L collapse on top of each other when the data aer rescaled using the critical exponents $\gamma = 1.819 \pm 0.003$ [32] and $\nu = 0.875 \pm 0.001$ [33] of standard three-dimensional (3D) percolation. Additionally, in Sec. II of the Supplemental Material [30] it is shown that there is a slight dependence on the percolation order near the critical

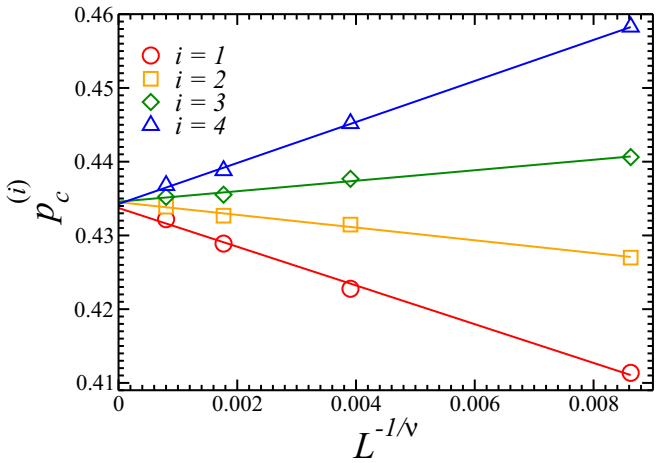


FIG. 3. Percolation threshold p_c as a function of $L^{-1/\nu}$ for four different species. For each realization, we record $p_c^{(i)}$ as the fraction p of chosen bonds when the ith percolation transition takes place. In case more than one cluster of same species connects the boundaries, we record the first one percolating. The values of $p_c^{(i)}$ are the average of these percolation thresholds over 1000 realizations, for $L = 64$, and over 100 realizations for $L = 128$, 256, and 512. Here, we considered four species and the initial density $\rho = 0.025$, values for which we always find four percolating species for all investigated system sizes. The curves follow a function given by Eq. (2) and the extrapolation of the straight lines suggests that in the thermodynamic limit, $L \to \infty$, all the clusters percolate at the same fraction $p_c = 0.434 \pm 0.001$. The statistical errors are smaller than the size of the symbols and were therefore omitted from the figure. Here, we used the value of the exponent $\nu = 0.875 \pm 0.001$ of standard 3D percolation [33].

point and we present two figures that replicate the analysis for the case of eight species: one for a simple cubic lattice and another for a cubic lattice with bonds between nearest neighbors and second nearest neighbors (2NN) [34].

Figure 3 presents the variation of the percolation thresholds $p_c^{(i)}$ as a function of $L^{-1/\nu}$, where $i = 1, 2, 3, 4$ corresponds to four species. These thresholds indicate the point at which the ith species exhibits a cluster that spans from the top to the bottom faces of the system. We observe that the values of $p_c^{(i)}$ for all species tend to converge to the same point as the lattice size increases. The least-squares fit to the data of each curve is consistent with the following equation [35],

$$p_c^{(i)}(L) = p_c\left(1 - a_i L^{-\frac{1}{\nu}}\right), \tag{2}$$

where a_i takes different values for different species and extrapolating $L \to \infty$ gives $p_c = 0.434 \pm 0.001$, a result that is consistent with the scaling shown in the upper inset of Fig. 2. Note that the value obtained is much larger than the threshold of classical percolation on the simple cubic lattice, $p_c = 0.248\,812\,6 \pm 0.000\,000\,5$ [33]. However, we observe that, in our model, p_c increases linearly with ρ and exponentially with k (see Sec. III of the Supplemental Material [30]).

Next, we study the fractal dimension of these percolating clusters segregated by the percolation order i. In fact, we considered for each species the size of the largest cluster at the extrapolated critical threshold $p_c = 0.434 \pm 0.001$ [36,37]. Then we define as M_i the mass of the cluster of the species which percolates at the ith threshold $p_c^{(i)}$, averaged over 1000 realizations. As can be seen in Sec. IV of the Supplemental Material [30], the results suggest that, at the critical point p_c the least-squares fit to the cluster mass M_i follows a power law [38]

$$M_i = b_i L^{d_f}, \tag{3}$$

where, within error bars, the fractal dimension d_f is consistent with the fractal dimension of the spanning cluster of classical percolation in 3D, $d_f = 2.5226 \pm 0.0001$ [39]. Additionally, the prefactors b_i decrease with the percolation order i following an exponential behavior,

$$b_i = Ae^{-Bi}, \tag{4}$$

where the least-squares fit to the data using Eq. (4) gives $A = 0.75 \pm 0.01$ and $B = 0.24 \pm 0.02$, showing that the average masses of largest clusters at p_c decrease with their percolation order i.

In order to achieve the simultaneous percolation of multiple species, it is not only necessary to set adequate values for the system size L and the number of species k, but crucially also to choose the appropriate initial density ρ. Given the system size L and the number of species k, the values of ρ for which the maximum number k of percolating clusters can be achieved is bound from below and from above: $\rho_{\min} < \rho < \rho_{\max}$. When the initial density ρ is below $\rho_{\min}$, we observe that one or more species never percolate. We also found that $\rho_{\min}$ decreases exponentially with k and decreases with L following a power law.

Since the threshold for site percolation on a simple cubic lattice is $p_c = 0.311\,607\,68 \pm 0.000\,000\,15 < 1/3$ [40], one obtains simultaneous percolating clusters for $k = 2$ and $k = 3$ even if all sites are inhabited from the beginning ($\rho k = 1$), as in the polychromatic model [17]. On the other hand, if $k > 3$ there exists a $\rho_{\max} < 1/k$ above which clusters hinder each other from growing because there are too few uninhabited nodes for the growing clusters to aggregate. At this density value $\rho_{\max}$, there is a transition from a situation where all species percolate to a situation at which none of the species percolates. As the system size L increases, this transition in ρ becomes more pronounced following a finite-size scaling in $L^{-1/\nu}$, with $\nu = 0.875 \pm 0.001$ being the value of standard 3D percolation [33], suggesting that it is a classical percolation transition. More details are given in Sec. V of the Supplemental Material [30]. We find that increasing k the value of $\rho_{\max}$ decreases exponentially as

$$\rho_{\max} = A_{\max} e^{-\alpha_{\max} k}. \tag{5}$$

The least-squares fit to the data using this exponential law gives $A_{\max} = 3.93 \pm 0.01$ and $\alpha_{\max} = 0.80 \pm 0.01$. This is shown in the lower inset of Fig. 4.

Next, we looked for the minimum lattice size $L_{\min}$ required to obtain k percolating clusters of different species. These results are illustrated in Fig. 4. Each point of this plot was obtained by finding the value of $L_{\min}$ for which there were k percolating clusters of different species in all realizations. The curve presented follows an exponential law,

$$L_{\min} = A_L e^{\alpha_L k}. \tag{6}$$

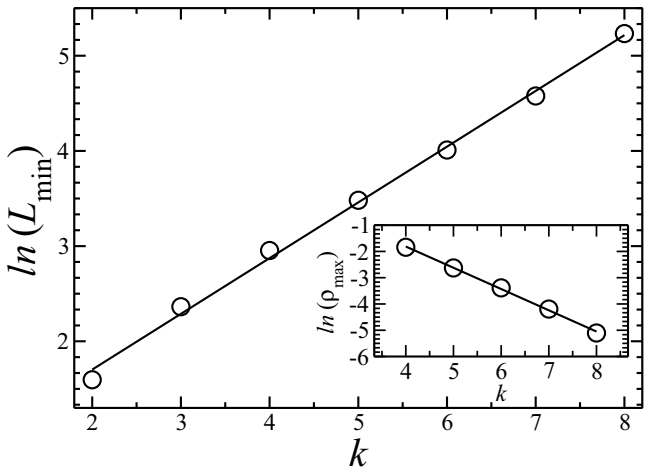


FIG. 4. Semilogarithmic plot of the minimum lattice side length $L_{\min}$ required to obtain k percolating clusters of different species. Data are obtained in the following way: For each number of species k ranging from 2 to 8, we searched for the minimum side length $L_{\min}$ for which every species percolated across 100 realizations. $L_{\min}$ increases exponentially with k, as expressed in Eq. (6). In the inset, we show, in a semilogarithmic plot, that $\rho_{\max}$ decreases exponentially with k following Eq. (5). In all cases, the errors were found to be smaller than the size of the symbols.

The least-squares fit to the data using Eq. (6) gives $A_L = 1.70 \pm 0.01$ and $\alpha_L = 0.59 \pm 0.01$. Interestingly, this expression shows that we can achieve percolation for as many clusters as we want, as long as we have a sufficiently large lattice.

The results presented up to now were obtained on simple cubic lattices with bonds only between nearest neighbors (NN). We observed that exponential relations such as those of Eqs. (5) and (6), although with different numerical values of parameters, are also valid for diamond lattices [41] and cubic lattices with bonds between nearest neighbors and second nearest neighbors (2NN) [34]. This implies that these parameters are not universal but depend on the lattice structure.

In this Letter, we have shown that our model allows for the existence of an unlimited number of percolating clusters both at and above the critical point. We found that the minimum lattice size $L_{\min}$ required to achieve a specific number of percolating clusters k grows exponentially with k. In other words, if we have a sufficiently large lattice, we can achieve as many percolating clusters as desired. The multiple percolation transitions all seem to have the same critical exponents as 3D classical percolation and thus to belong to the same universality class. Furthermore, this model can also be studied in other situations, such as when ρ is not the same for every species. The findings of our study strongly suggest that it should be possible to experimentally realize objects exhibiting multiple percolating clusters such as trigels, tetragels, and so on. More details of this work will be addressed in a future publication.

We are thankful for the financial support from the Brazilian agencies CNPq, CAPES, FUNCAP and the National Institute of Science and Technology for Complex Systems (INCT-SC). This work was also partly supported by the Research Council of Norway through its Center of Excellence funding scheme, Project No. 262644. Further support, also from the Research Council of Norway, was provided through its INTPART program, Project No. 309139. A.H. furthermore acknowledge funding from the European Research Council (Grant Agreement No. 101141323 AGIPORE).

[1] A. Fernandez-Nieves and A. M. Puertas, *Fluids, Colloids and Soft Materials: An Introduction to Soft Matter Physics* (Wiley, Hoboken, NJ, 2016).

[2] L. Di Michele, D. Fiocco, F. Varrato, S. Sastry, E. Eiser, and G. Foffi, Aggregation dynamics, structure, and mechanical properties of bigels, Soft Matter **10**, 3633 (2014).

[3] F. Varrato, L. Di Michele, M. Belushkin, N. Dorsaz, S. H. Nathan, E. Eiser, and G. Foffi, Arrested demixing opens route to bigels, Proc. Natl. Acad. Sci. USA **109**, 19155 (2012).

[4] B. Verhaeghe, F. Louchet, Y. Bréchet, and J. Massoud, Damage and rupture mechanisms in a bipercolated material: The example of austenoferritic duplex steels, Mater. Sci. Eng. A **234–236**, 279 (1997).

[5] N. Zhang, W. Li, C. Chen, and J. Zuo, Molecular dynamics simulation of aggregation in dimethyl sulfoxide–water binary mixture, Comput. Theor. Chem. **1017**, 126 (2013).

[6] Y. Shao, Z. xuan Yang, B. wen Deng, B. Yin, and M. bo Yang, Tuning PVDF/PS/HDPE polymer blends to tri-continuous morphology by grafted copolymers as the compatibilizers, Polymer **140**, 188 (2018).

[7] Z. Gan, C. Zhang, Z.-R. Zhang, Z.-J. Chen, and L. Liu, Crystallization-dependent transition of corrosion resistance of an Fe-based bulk metallic glass under hydrostatic pressures, Corros. Sci. **179**, 109098 (2021).

[8] M. Aizenman, On the number of incipient spanning clusters, Nucl. Phys. B **485**, 551 (1997).

[9] C. I. N. Sampaio Filho, J. S. Andrade, H. J. Herrmann, and A. A. Moreira, Elastic backbone defines a new transition in the percolation model, Phys. Rev. Lett. **120**, 175701 (2018).

[10] W. R. d. Sena, J. S. Andrade, H. J. Herrmann, and A. A. Moreira, Decomposing the percolation backbone reveals novel scaling laws of the current distribution, Front. Phys. **11**, 1335339 (2023).

[11] C. Newman and L. Schulman, Infinite clusters in percolation models, J. Stat. Phys. **26**, 613 (1981).

[12] C. Newman and L. Schulman, Number and density of percolating clusters, J. Phys. A: Math. Gen. **14**, 1735 (1981).

[13] J. Cardy, The number of incipient spanning clusters in two-dimensional percolation, J. Phys. A: Math. Gen. **31**, L105 (1998).

[14] P. Grassberger and W. Nadler, 'Go with the winners' simulations, in *Computational Statistical Physics: From Billiards to Monte Carlo* (Springer, Berlin, 2002), pp. 169–190.

[15] D. Aldous and U. Vazirani, "Go with the winners" algorithms, in *Proceedings 35th Annual Symposium on Foundations of Computer Science* (IEEE, New York, 1994), pp. 492–501.

[16] L. N. Shchur and T. Rostunov, On the Aizenman exponent in critical percolation, JETP Lett. **76**, 475 (2002).

[17] R. Zallen, Polychromatic percolation: Coexistence of percolating species in highly connected lattices, Phys. Rev. B **16**, 1426 (1977).
[18] M. Giona and A. Adrover, Multicomponent percolation: Probabilistic properties and application to nonisothermal reactions in granular materials, Phys. Rev. E **49**, 5287 (1994).
[19] A. S. Ioselevich, Multicomponent percolation criterion and its application to hopping in disordered conductors, Phys. Rev. Lett. **74**, 1411 (1995).
[20] H. M. Harreis and W. Bauer, Phase transitions in a two-component site-bond percolation model, Phys. Rev. B **62**, 8719 (2000).
[21] I. V. Petrov, I. I. Stoynev, and F. V. Babalievskii, Correlated two-component percolation, J. Phys. A: Math. Gen. **24**, 4421 (1991).
[22] J. Lin, *A Generalized Model for Site Percolation with Two Independent Concentrations*, Tech. Rep. No. IC–87/63 (International Centre for Theoretical Physics, Vienna, 1987).
[23] J. C. Wierman, AB percolation: A brief survey, Banach Center Publ. **25**, 241 (1989).
[24] H. Kesten and Z. Su, Some remarks on *AB*-percolation in high dimensions, J. Math. Phys. **41**, 1298 (2000).
[25] S. Kundu and S. S. Manna, Colored percolation, Phys. Rev. E **95**, 052124 (2017).
[26] V. Avetisov, A. Gorsky, S. Nechaev, and O. Valba, Spontaneous symmetry breaking and phase coexistence in two-color networks, Phys. Rev. E **93**, 012302 (2016).
[27] V. Avetisov, A. Gorsky, S. Nechaev, and O. Valba, Finite plateau in spectral gap of polychromatic constrained random networks, Phys. Rev. E **96**, 062309 (2017).
[28] R. M. Bradley, P. N. Strenski, and J.-M. Debierre, A growing self-avoiding walk in three dimensions and its relation to percolation, Phys. Rev. A **45**, 8513 (1992).
[29] M. E. J. Newman and R. M. Ziff, Efficient Monte Carlo algorithm and high-precision results for percolation, Phys. Rev. Lett. **85**, 4104 (2000).
[30] See Supplemental Material at http://link.aps.org/supplemental/10.1103/PhysRevResearch.7.L022067 for an illustration of the model rules, details on the second moment, the dependence of the critical point on initial density and number of species, the fractal dimension, and the maximum density.
[31] D. Stauffer and A. Aharony, *Introduction to Percolation Theory* (Taylor and Francis, 1991).
[32] S. Fayfar, A. Bretaña, and W. Montfrooij, Protected percolation: A new universality class pertaining to heavily-doped quantum critical systems, J. Phys. Commun. **5**, 015008 (2021).
[33] C. D. Lorenz and R. M. Ziff, Precise determination of the bond percolation thresholds and finite-size scaling corrections for the sc, fcc, and bcc lattices, Phys. Rev. E **57**, 230 (1998).
[34] Z. Xun and R. M. Ziff, Bond percolation on simple cubic lattices with extended neighborhoods, Phys. Rev. E **102**, 012102 (2020).
[35] L. Böttcher and H. J. Herrmann, *Computational Statistical Physics* (Cambridge University Press, Cambridge, UK, 2021).
[36] P. Sen, Nature of the largest cluster size distribution at the percolation threshold, J. Phys. A: Math. Gen. **34**, 8477 (2001).
[37] N. Jan, D. Stauffer, and A. Aharony, An infinite number of effectively infinite clusters in critical percolation, J. Stat. Phys. **92**, 325 (1998).
[38] A. Kapitulnik, A. Aharony, G. Deutscher, and D. Stauffer, Self similarity and correlations in percolation, J. Phys. A: Math. Gen. **16**, L269 (1983).
[39] Y. Deng and H. W. J. Blöte, Monte Carlo study of the site-percolation model in two and three dimensions, Phys. Rev. E **72**, 016126 (2005).
[40] X. Xu, J. Wang, J.-P. Lv, and Y. Deng, Simultaneous analysis of three-dimensional percolation models, Front. Phys. **9**, 113 (2014).
[41] C. Kittel and P. McEuen, *Introduction to Solid State Physics* (Wiley, Hoboken, NJ, 2018).